

Case Report

# Comparative Assessment of Biochar Stability Using Multiple Indicators

Keiji Jindo <sup>1</sup> and Tomonori Sonoki <sup>2,\*</sup>

<sup>1</sup> Plant Production System Group, Wageningen University and Research, 6708PB Wageningen, The Netherlands; keijindo@gmail.com

<sup>2</sup> Faculty of Agriculture and Life Science, Hirosaki University, Aomori 036-8560, Japan

\* Correspondence: sonoki@hirosaki-u.ac.jp; Tel.: +81-172-39-3585

Received: 18 April 2019; Accepted: 18 May 2019; Published: 21 May 2019



**Abstract:** Biochar application is one strategy proposed to improve carbon sequestration in soil. Maintaining high carbon content in soil for a long period requires stable biochar. In this work, we assessed biochar stability by two methodologies, i.e., laboratory incubation and chemical oxidation. Biochar was produced at four different temperatures (400 °C, 500 °C, 600 °C, and 800 °C) from rice (*Oryza sativa* L.) straw and husk, applewood branch (*Malus pumila*), and oak (*Quercus serrata* Murray) residues. Results showed that the high-temperature biochars were more stable in both abiotic and biotic incubations, whereas the low-temperature biochars had reduced longevity. In addition, we showed biochars originated from woody material have higher stable carbon than those produced from rice residues. Finally, the oxidative assessment method provided a more reliable estimation of stability than the biotic incubation method and showed a strong correlation with other stability indicators.

**Keywords:** biochar; stability; pyrolysis; rice straw; rice husk

## 1. Introduction

Carbon sequestration in soil is one of the strategies used to mitigate climate change associated with greenhouse gas emissions. The Intergovernmental Panel on Climate Change (IPCC) produced a special report on global warming of 1.5 °C (<http://www.ipcc.ch/report/sr15/>) and proposed the application of biochar to soil as a promising negative emission technology [1]. To extensively and successfully implement this technology, the properties of biochar must first be more fully understood. The interdependency between the types of feedstock and the pyrolysis processes determine biochar properties, and this, in turn, impacts the stability of biochar in soil. Biochar degradation is of interest not only with regard to soil carbon sequestration but also because of the potential for application as a bulk agent to enhance the composting process. Decisions on the use of biochar are linked to the properties that affect biochar stability [2]. Methodologies for estimation of biochar stability have been described in several review reports [3–7]. Three categories that define biochar stability include (1) carbon structure; (2) labile/stable carbon; and (3) biotic-abiotic mineralization in incubation and modeling. Of these, incubation and modeling is the preferred option for estimating biochar degradation because the results are directly linked to the recalcitrance of biochar in soil. However, other indicators (e.g., H:C ratio) are practically used as proxies to test for stability because they eliminate the need for time-consuming incubation studies in soil [5]. One of the most cost-effective and relatively rapid methods used to test stability is the H<sub>2</sub>O<sub>2</sub>- and heat-assisted oxidation method, which is often called the “Edinburgh stability tool” proposed by Cross and Sohi [8]. This simulation of oxidative degradation in soil is considered a reliable approach by other researchers [9–11]. As a follow up to our previous work [12], we assessed the carbon stabilities of four types of biochars prepared from rice straw (RS), rice husk

(RH), and two woody plants, oak (*Quercus serrate Murray*) (OB) and applewood branch (*Malus pumila*) (AB), by means of the aforementioned incubation and oxidative method.

## 2. Materials and Methods

### 2.1. Pyrolysis Process for Biochar Preparation

Four different feedstocks were used for biochar production. These included two woody materials, oak (*Quercus serrate Murray*) and applewood branch (*Malus pumila*), plus rice residues (*Oryza sativa L.*) of straw and husk. The materials were cut into small pieces less than 4–5 cm, air-dried, and then pyrolyzed in an electric furnace (SOMO-01 Isuzu, Japan) to prepare for biochar. The furnace temperature was increased from room temperature with a heating rate of  $10\text{ }^{\circ}\text{C min}^{-1}$  to four different temperatures (400 °C, 500 °C, 600 °C, and 800 °C) and then maintained for 10 h for pyrolysis.

### 2.2. Biochar Chemical Analysis

All biochars were ground and sieved to less than 0.5 mm in diameter. The volatile matter content (%) and ash content (%) were determined by measuring the weight loss through heat treatment (950 °C, 7 min for volatile, and 750 °C, 6 h for ash) of ca. 1 g each of biochar in a crucible. Fixed carbon contents (%) were calculated as follows: the total mass of biochar minus the sum of volatile ash and moisture content. Acid function group was measured based on the titration method using NaOH (0.01 M) and HCl (0.05 M). The detection limit of the acid functional group was 0.01 mmol/g. The elementals, C, H, and N were determined using a Thermo Finnigan EA-1112 analyzer (Thermo Fisher Scientific Inc., MA, USA); O was determined with the vario El cube (Elementar Analysensysteme GmbH). Cross-Polarization/Magic Angle Spinning (CPMAS)  $^{13}\text{C}$  Nuclear Magnetic Resonance ( $^{13}\text{C}$ -NMR) spectra were acquired from the solid samples with a Varian 300, equipped with a 4 mm wide bore MAS probe, operating at a  $^{13}\text{C}$  resonating frequency of 75.47 MHz. The spectra were integrated into the chemical shift (ppm) resonance intervals of alkyl-C (0–45 ppm), O-alkyl-C (45–110 ppm), olefinic, phenolic, aromatic-C (110–160 ppm), and carbonyl C (160–210 ppm). The degree of aromaticity (%) was calculated as follows [13]:  $\text{aromatic-C} \times 100 / (\text{alkyl-C} + \text{O-alkyl-C} + \text{aromatic-C})$ . Thermal analyses were conducted under a static-air atmosphere as follows: a temperature equilibrating at 30 °C followed by a linear heating rate of  $5\text{ }^{\circ}\text{C min}^{-1}$  from 30 °C to 105 °C at which point, an isotherm was maintained for 10 min, and then ramping continued at  $5\text{ }^{\circ}\text{C min}^{-1}$  from 105 °C to 680 °C. The ash content was calculated from the inorganic residue remaining at the end of the ramping period. The main weight losses occurred in the 110 °C to 350 °C (W1) and 350 °C to 550 °C (W2) ranges. The ratio W2/W1 was deployed as a thermal lability index of the organic materials [14].

### 2.3. Estimation of Biochar Stability

#### 2.3.1. Incubation Method: Biotic and Abiotic Degradation

The stability of each biochar type against microbial degradation was assessed by the incubation method [15]. Twenty milligrams of biochar dry matter was mixed with 200 mg of quartz sand in a screw-cap tube ( $\varphi 18 \times 180$  mm) and sterilized (121 °C, 20 min). Soil (10 g) from the Campus of Hirosaki University was suspended in 100 mL of deionized water and stirred continuously at room temperature. After 1 h, the suspension was stated for 30 min without stirring and then the supernatant was used as the inoculum for the biotic incubation. Next, 20 microliters of the inoculum and 80  $\mu\text{L}$  of the nutrient solution [60 g/L  $(\text{NH}_4)_2\text{SO}_4$ , 6 g/L  $\text{KH}_2\text{PO}_4$ , 7.7 g/L  $\text{K}_2\text{HPO}_4$ ] were mixed with the biochar and quartz sand in the screw-cap tube then sealed with a butyl rubber stopper-assembled screw-cap, and incubated at 30 °C (biotic incubation). Sterile water was added instead of the inoculum to monitor microbial degradation-independent  $\text{CO}_2$  emission from the biochar (abiotic incubation). The concentration of  $\text{CO}_2$  in the screw-cap tube was periodically measured using a gas chromatograph (GC, Agilent 7890A Valve system, Agilent Technologies Inc.) equipped with an HP-PLOT/Q column (Agilent Technologies

Inc). The oven was maintained at 50 °C and helium was used as the carrier (3.5 mL/min). Pulsed Discharge Helium Ionization Detector was used and kept at 120 °C. The cumulative mineralized C and mineralization rate was calculated by using the Equations (1) and (2), respectively [15].

$$\text{Cumulative mineralized C (mg C/g Biochar)} = (D_t - D_0) \times (12/44)/S \quad (1)$$

$D_t$ : CO<sub>2</sub> (mg) at t days during the incubation

t: days elapsed from the start of the incubation (1, 2, 4, 8, 16, 32, 64, and 120)

$D_0$ : CO<sub>2</sub> (mg) at the start of incubation

12: the atomic mass of carbon

44: the atomic mass of CO<sub>2</sub>

S: biochar amount (g)

$$\text{Mineralization rate (mg C/g biochar/year)} = \text{cumulative mineralized C}/t/365 \quad (2)$$

t: days elapsed from the start of the incubation (1, 2, 4, 8, 16, 32, 64, and 120)

### 2.3.2. Chemical Oxidation Method: Abiotic Degradation (“Edinburgh Stability Tool”)

Biochar stability was also assessed using the chemical oxidation method, “Edinburgh stability tool” [8]. All biochar samples were heat-dried at 105 °C for more than 12 h. Based on the carbon content from the elemental analysis, the biochar containing 0.1 g of carbon was weighed and mixed with 7 mL of 5% H<sub>2</sub>O<sub>2</sub> in a screw-cap tube (φ16 × 125 mm). The tubes were tightly capped and kept at 80 °C for 48 h and then cooled to room temperature. The solid residue was collected with a quantitative filter paper (No. 5C) and heat-dried at 105 °C for more than 12 h after washing several times with sterile water. The carbon content in the dried residue was determined as described above. The stable carbon was calculated by the following Equation (3):

$$\text{Stable carbon (\%)} = \frac{\{\text{Carbon (g) after 5\% H}_2\text{O}_2 \text{ treatment}\}}{\{\text{Carbon (g) before 5\% H}_2\text{O}_2 \text{ treatment}\}} \times 100 \quad (3)$$

### 2.4. Correlation Among Stability Indicators

Correlation between biochar stability indicators was evaluated. H:C ratio, O:C ratio, degree of aromaticity, volatile content: fixed carbon ratio, Edinburgh stability tool, abiotic incubation, and total (biotic + abiotic) incubation were included. Additionally, the feedstock of the biochar material, the pyrolysis temperature and ash content, were used in the correlation analysis to analyze the relationship with the indicators. The feedstock was considered as a binary variable (1 = Woody materials (AB and OB), 0 = Rice materials (RH and RS)). For the incubation experiments, data for the 32nd day, when the CO<sub>2</sub> cumulative started to decline, were used for the correlation. The order of the correlation matrix was arranged based on the hierarchical clustering of correlation coefficients by using “corrplot package” in Rstudio program.

### 2.5. Statistical Analysis

All of the experiments were conducted in duplicate or triplicate, and the average values were reported. The statistical analyses were conducted with R program (Rstudio 3.5.1 version, RStudio, Boston, MA, USA), and the significant differences were verified at  $p < 0.05$ .

## 3. Results and Discussion

### 3.1. Chemical and Physical Characteristics of Biochars

The percentages of volatile, ash, and fixed carbon contents are shown in Table 1. Volatile content decreased and ash content increased with increasing pyrolysis temperature. The biochars from rice

residues (RH and RS) showed greater ash content than those from woody materials (AB and OB) due to the existence of high mineral (e.g., Si) content. High-ash biochars enriched with alkaline elements can be a potentially applicable material for plant growth [2,16]. The biochars from woody materials (AB and OB) have a higher content of fixed carbon than those from rice residues (RH and RS). Acid functional group contents were significantly higher in the biochars that pyrolyzed at the lowest temperature in our study (400 °C). As the pyrolysis temperature increased, aromaticity increased across all feedstock types, peaked at 600 °C and then declined at 800 °C. Increasing the pyrolysis temperature lowered easily-degradable carbon content and created a tolerant aromatic structure. All biochars showed increasing ratios of W2/W1 with increasing temperatures, suggesting a more stable chemical structure remained [5–8,17,18]. Increasing temperatures up to 600 °C resulted in a higher aromatic carbon proportion due to the volatilization of aliphatic groups, and this alteration makes the biochar resistant to microbial decomposition (Table 1). However, further increases in pyrolysis temperature from 600 °C to 800 °C changed the chemical structure, reducing aromaticity and the W2/W1 ratio. A similar trend was noted in another report [2] when the temperature was increased to 750 °C, resulting in the loss of aromatic groups due to the high-temperature. As an organic amendment to improve soil nutrition, the use of the low-temperature (400 °C) biochars having easily-biodegradable carbons would be favorable for plant growth by stimulating soil microorganisms [19,20]. On the other hand, biochars pyrolyzed at 600 °C and enriched with recalcitrant chemical composition would be more suitable not only for carbon sequestration via the use in composting or soil amendment but also for N<sub>2</sub>O reduction during composting [2].

**Table 1.** Physical and chemical characteristics of biochar from different feedstocks: AB (applewood branch), OB (oak), RH (rice husk), and RS (rice straw).

Materials	Temperature (°C)	Volatile Content (%) <sup>4</sup>	Ash Content (%) <sup>4</sup>	Fixed Carbon (%) <sup>1</sup>	Acid Functional Group (mmol/g) <sup>4</sup>	Degree of Aromaticity <sup>2</sup> (%)	W2/W1 <sup>3</sup>
AB	400	32.36 ± 0.05	4.37 ± 0.04	63.3	0.34 ± 0.05	55.2	2.6
	500	18.27 ± 0.28	6.45 ± 0.13	74.5	N.D.	67.9	10.2
	600	11.07 ± 0.20	7.61 ± 0.07	81.3	N.D.	72.8	14.6
	800	6.82 ± 0.07	8.58 ± 0.02	84.8	N.D.	63.9	22.9
OB	400	32.06 ± 0.05	3.63 ± 0.02	64.3	0.32 ± 0.00	56.8	4.6
	500	19.42 ± 0.27	5.10 ± 0.12	75.5	0.13 ± 0.28	66.7	10.0
	600	12.30 ± 0.01	5.54 ± 0.02	82.2	0.02 ± 0.20	73.2	21.7
	800	7.87 ± 0.06	8.25 ± 0.23	84.0	N.D.	62.1	15.7
RH	400	22.00 ± 0.13	35.9 ± 0.06	42.1	0.58 ± 0.05	61.5	3.1
	500	10.56 ± 0.11	46.2 ± 0.23	43.2	0.26 ± 0.05	64.8	10.9
	600	6.02 ± 0.27	52.8 ± 0.41	41.2	0.11 ± 0.00	72.4	18.0
	800	3.17 ± 0.19	62.6 ± 0.26	34.2	N.D.	54.0	18.0
RS	400	22.42 ± 0.09	34.0 ± 0.18	43.5	0.51 ± 0.03	54.2	1.8
	500	12.80 ± 0.11	40.0 ± 0.31	43.9	N.D.	63.1	4.3
	600	8.36 ± 0.03	58.6 ± 0.07	33.0	N.D.	68.2	4.6
	800	4.47 ± 0.15	73.9 ± 0.05	21.6	N.D.	44.9	4.2

<sup>1</sup> Fixed carbon: the total mass of biochar minus the sum of volatile, ash and moisture content; <sup>2</sup> Degree of aromaticity = aromatic-C × 100/(alkyl-C + O-alkyl-C + aromatic-C); <sup>3</sup> Ratio between the mass losses associated with the second (W2) and first (W1) exothermic reactions of thermal analysis; <sup>4</sup> Each value is the average ± the standard deviation from three independent experiments.

### 3.2. Evaluation of Biochar using Incubation Methods

Figures 1 and 2 represent the cumulative mineralized carbon and mineralization rate of the four biochars under (a) abiotic and (b) total (biotic + abiotic) incubation, respectively. In every case, the amount of mineralized carbon decreased with increasing pyrolysis temperature. In the latter incubation, the mineralization clearly increased over time and the highest cumulative mineralized carbon was observed in the lowest-temperature biochars pyrolyzed at 400 °C (AB-400 °C, OB-400 °C, RH-400 °C, and RS-400 °C), probably due to the presence of the volatile content and acid functional

group for microbial activity (Table 1). Peng et al. [21] reported that low-temperature biochar had easily-biodegradable components such as aliphatic carbons, carboxylic acids, and carbohydrates, and further showed a high correlation between the volatile contents and mineralization rates [21]. AB- and OB-biochars showed lower carbon releases than RH- and RS-biochars due to the fixed carbon contents (Figure 1). It would be interesting to use this method with the extract from composting material to detect possible microbial degradation during the composting process, given that volatile compounds derived from biochar were closely related to the microbial community for decomposition during the composting process [22].

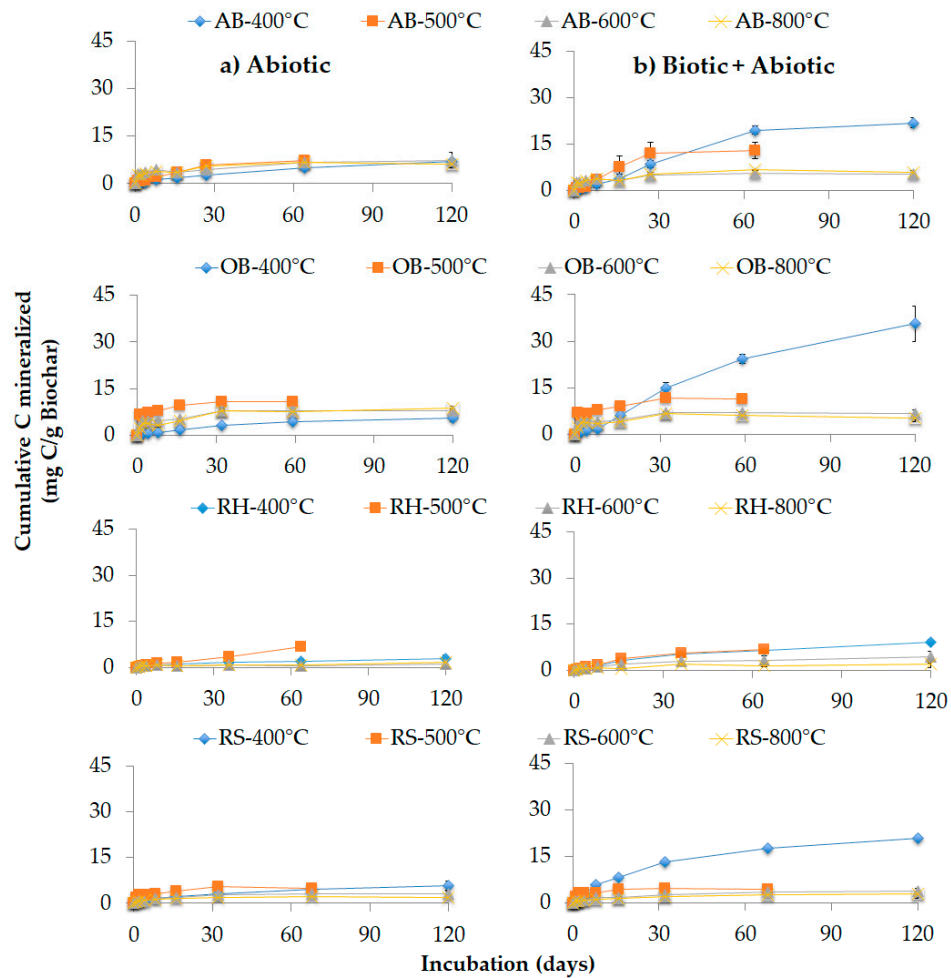


**Figure 1.** Cumulative carbon mineralized during 120 days under abiotic (a) and total (biotic + abiotic) (b) incubations of biochars from different feedstocks: AB (applewood branch), OB (oak), RH (rice husk), and RS (rice straw). Each error bar represents the standard deviation from three independent experiments.

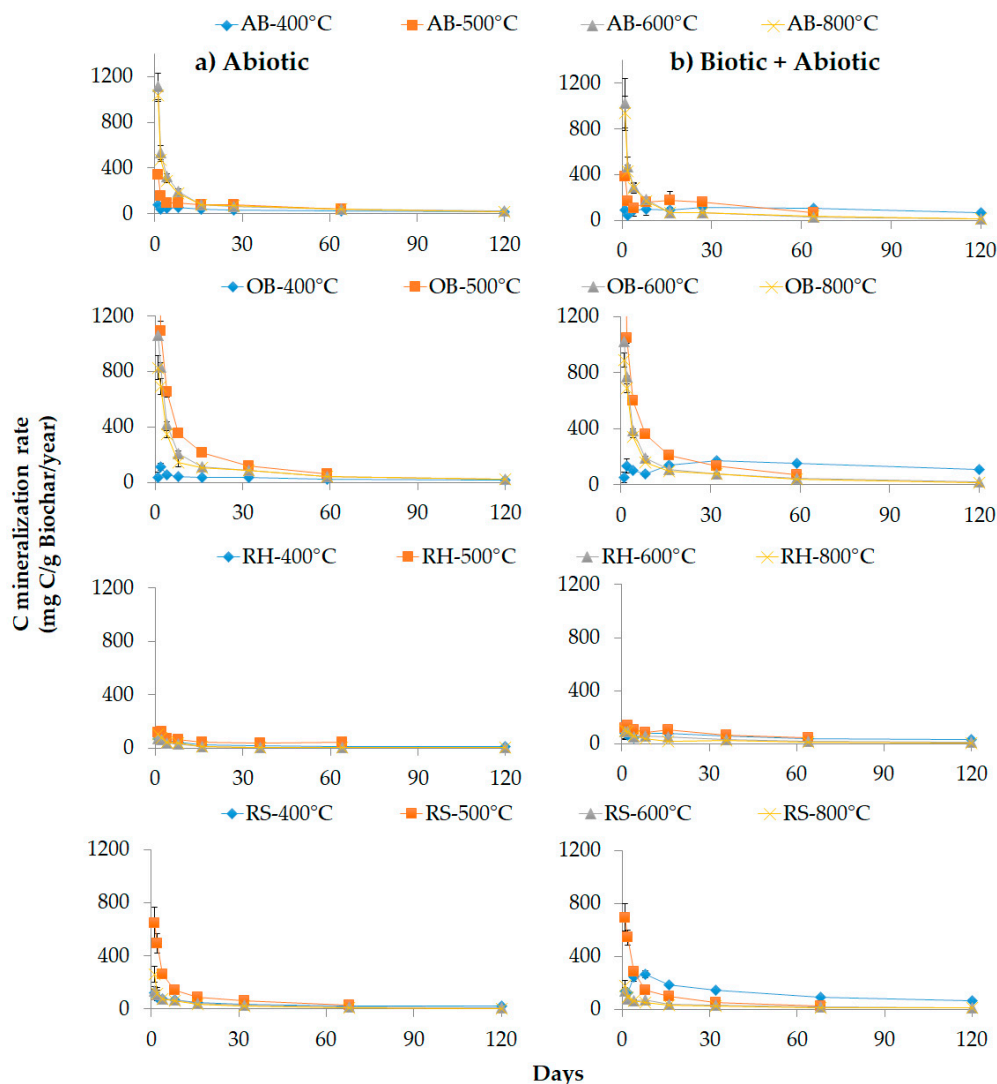


**Figure 2.** C-mineralization rate per year of biochars under abiotic (a) and total (biotic + abiotic) (b) incubations of biochars from different feedstocks: AB (applewood branch), OB (oak), RH (rice husk), and RS (rice straw). Each error bar represents the standard deviation from three independent experiments.

The results from the abiotic incubations showed similar trends of mineralization when compared with biotic + abiotic incubation (Figure 2, right). Relationships between the mineralization rates and the incubation durations are shown in Figure 3. Generally, high correlations were confirmed in all cases (Figure 3), especially in the high-temperature biochars under both incubations. On the other hand, negligible correlation or a weak correlation was shown ( $0.03 < R^2 < 0.37$ ) in the lowest-temperature biochars (AB-400 °C, OB-400 °C, RH-400 °C, and RS-400 °C) under biotic + abiotic incubation. Combining the results of the biotic + abiotic incubation (Figure 2) together with the fact that no correlation was obtained between the mineralization rates and the incubation days (shown in Figure 3), suggests a lack of biochar stability. The biotic method approaches are often criticized for the interdependency between soil properties and the soil microbial community [6], and thereby it is likely a suitable technique for site-specific research on biochar degradation, but not for comparative study under different biophysical conditions.

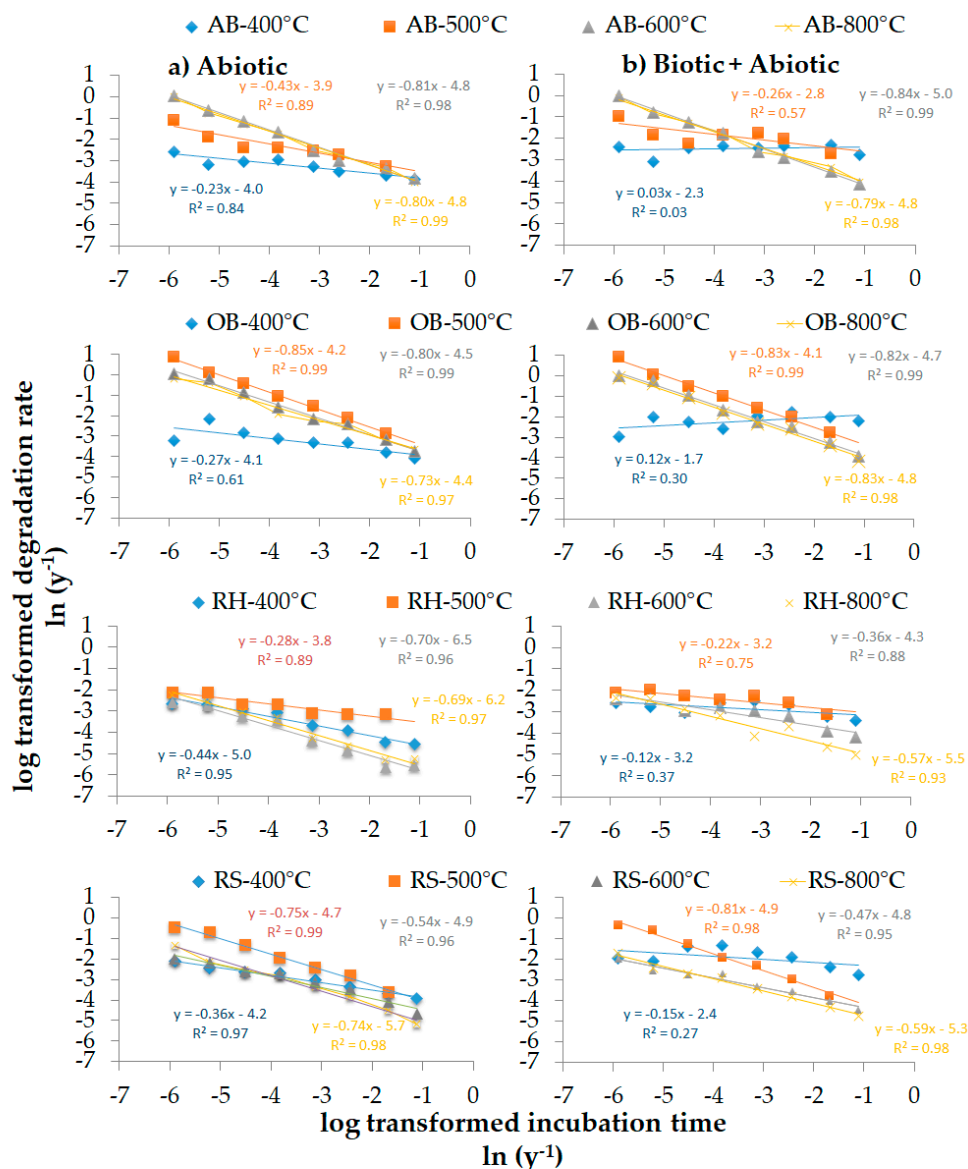


**Figure 3.** Correlation between the log transformed incubation time and log transformed degradation rate per year under abiotic (a) and total (biotic + abiotic) (b) incubations of biochars from different feedstocks: AB (applewood branch), OB (oak), RH (rice husk), and RS (rice straw).

### 3.3. Chemical Oxidation for Assessment of Biochar Stability

Comprehensive estimation of biochar stability was carried out by the chemical oxidation method proposed by Cross and Sohi [8]. The method is not affected by microbial inoculum, which is hard to control, and also makes it possible to measure carbon content that is relatively recalcitrant to the oxidation. The carbon stability calculated by this method is shown in Table 2. The stability of the biochar derived from woody materials (AB and OB) rose gradually with increasing temperature, with the highest-temperature biochar (800 °C) showing a 3- or 4-fold greater stability over those produced at 400 °C. Stable carbon of all biochars produced at 400 °C was ca. 20%, whereas those produced at 500 °C varied between 60%–100%. More than 80% of the stable carbon was estimated to remain in the biochars pyrolyzed at 600 °C and 800 °C. The increase of stable carbon aligned with that of the pyrolysis temperature in the case of woody-material biochars (AB and OB). In contrast, the stable carbon content of RH biochar increased at 400 °C, 500 °C, and 600 °C, but was reduced at 800 °C. For RS, the reduction in content was first observed when the pyrolysis temperature was 600 °C. These

results are similar to those reported in another paper [8]. It should be noted that the biochars originated from rice plant residues are enriched in ash, and would, therefore, be expected to trigger different outcomes of stable carbon compared with those from woody materials [16]. Of note, the total amount of crop residues produced worldwide is 3.8 Gt per year, of which 0.9 Gt derive from rice production (*Oryza sativa* L.) [23]. The main application of rice harvest residue around the world is as an amendment to the soil after burning the material on the field to preserve organic matter and nutrients, and this practice contributes significantly to GHG emissions. Alternatively, using rice residues as a biochar feedstock with subsequent application into the paddy rice soil is reported to have a positive impact on rice production in field experiments [24–26].

**Table 2.** Mean ( $n = 3$ ) and standard deviation  $\pm$  on the biochar stability (%) estimated by chemical oxidation method (“Edinburgh Stability Tool”) of the biochars from different feedstocks: AB (applewood branch), OB (oak), RH (rice husk), and RS (rice straw).

Materials	Stability (%)			
	400 °C	500 °C	600 °C	800 °C
AB	14.50 $\pm$ 0.24	69.35 $\pm$ 2.71	82.84 $\pm$ 0.36	84.63 $\pm$ 0.65
OB	21.72 $\pm$ 0.72	62.55 $\pm$ 1.11	86.09 $\pm$ 0.67	100.44 $\pm$ 1.13
RH	25.09 $\pm$ 0.24	63.35 $\pm$ 3.60	100.37 $\pm$ 3.72	84.72 $\pm$ 2.69
RS	19.52 $\pm$ 0.74	102.19 $\pm$ 1.99	81.76 $\pm$ 5.67	86.47 $\pm$ 6.30

### 3.4. Correlation

The degree of relationship between indicators is shown in Figure 4. The figure clearly shows the Edinburgh stability tool has a significant correlation with other indicators. Interestingly, the biotic + abiotic incubation shows more correlation with other stability indicators than the abiotic incubation. Pearson’s correlation coefficient ( $r$ ) of the Edinburgh stability tool with those incubation methods was 0.08 and  $-0.31$ , respectively. It is reported [5] that the linking between oxidative stability with the biotic and abiotic stability of biochar in soil is challenging, and more holistic studies need to be done. The H:C and volatile: fixed ratios have a tight relationship with other indicators such as O:C, W2/W1, and the Edinburgh stability tool. Moreover, the combination of these two indicators is proposed as a better approach for predicting stability [27]. The pyrolysis temperature has a strong or moderate correlation with all indicators except for aromaticity and abiotic incubation. The feedstock is strongly correlated with ash content ( $r = -0.93$ ) and moderately correlated with O:C ratio ( $r = -0.34$ ) and W2/W1 ( $r = 0.34$ ), implying the feedstock type of the biochar material affects the reliability of these indicators.

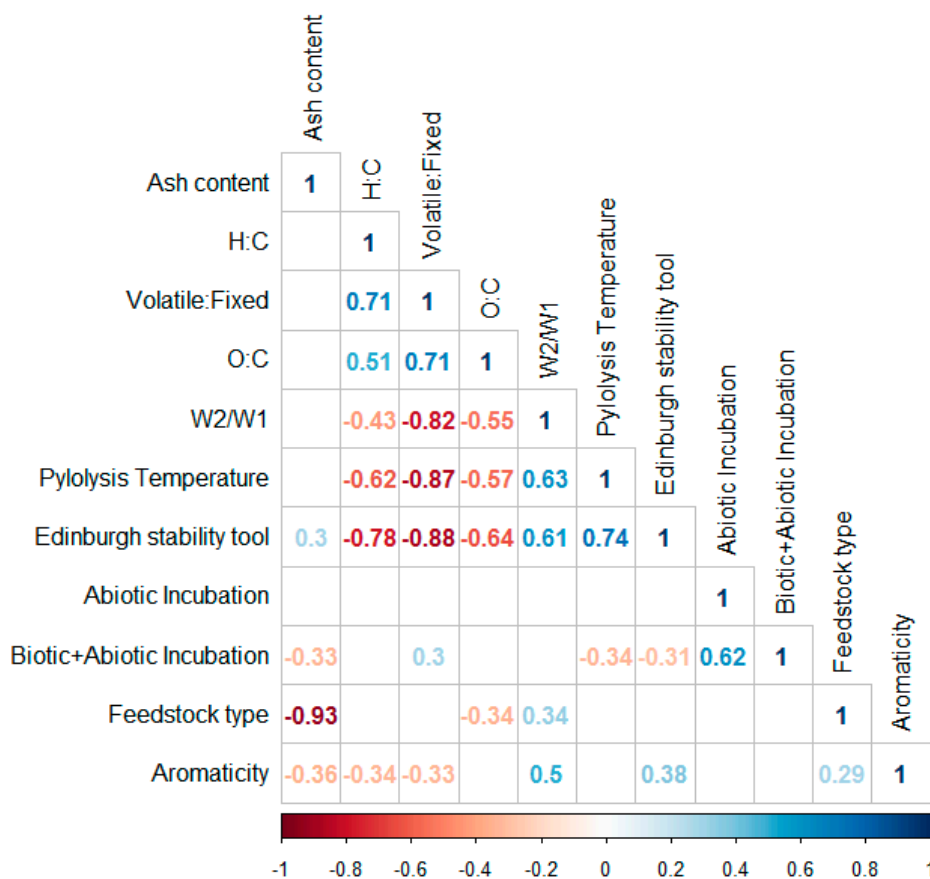


**Figure 4.** Correlation heatmap matrix of different stability indicators for biochar. Significance levels of Pearson correlation is 0.05. Blank means no significant coefficient. Blue number represents positive correlation, while red number represents negative correlation.

#### 4. Conclusions

We examined four biochar types and presented the results of the different stability indicators and their relationships. The “Edinburgh stability tool” oxidation method shows a tight relationship with other indicators across different types of feedstock. This method is easily implementable and comparable with other methods used to verify the stability of the biochar product. This method provides the means to select the correct product to meet agriculture and environmental objectives such as in composting or as an organic amendment. To ensure optimal N<sub>2</sub>O reduction during composting and high carbon sequestration in soil, the high-temperature (600 °C) biochars might be the suitable choice. The low-temperature (400 °C) biochars enriched with easily-biodegradable carbons would be more suitable for plant growth as an organic amendment.

**Author Contributions:** Conceptualization, K.J. and T.S.; methodology, T.S.; validation, T.S., formal analysis, K.J. and T.S.; investigation, K.J. and T.S.; data curation, K.J. and T.S.; writing—original draft preparation, K.J.; writing—review and editing, K.J. and T.S.; supervision, T.S.; funding acquisition, T.S.

**Funding:** This research was partly funded by a bilateral project of the Japan Society for the Promotion of Science (JSPS) and the Spanish National Research Council (CSIC).

**Acknowledgments:** This work was partly supported by the bilateral project of the Japan Society for the Promotion of Science (JSPS) and the Spanish National Research Council (CSIC). Special thanks to Mizumoto H, Hirosaki University and Sanchez-Monedero MA, CSIC-CEBAS for technical support.

**Conflicts of Interest:** The authors declare no conflict of interest.

## References

1. Alcalde, J.; Smith, P.; Haszeldine, R.S.; Bond, C.E. The potential for implementation of negative emission technologies in Scotland. *Int. J. Greenh. Gas Control* **2018**, *76*, 85–91. [[CrossRef](#)]
2. Domingues, R.R.; Trugilho, P.F.; Silva, C.A.; De Melo, I.C.N.A.; Melo, L.C.A.; Magriotis, Z.M.; Sánchez-Monedero, M.A. Properties of biochar derived from wood and high-nutrient biomasses with the aim of agronomic and environmental benefits. *PLoS ONE* **2017**, *12*, 1–19. [[CrossRef](#)]
3. Kurt, S. Review of the stability of biochar in soils: predictability of O:C molar ratio. *Carbon Manag.* **2010**, *1*, 289–303. [[CrossRef](#)]
4. Gurwick, N.P.; Moore, L.A.; Kelly, C.; Elias, P. A systematic review of biochar research, with a focus on its stability in situ and its promise as a climate mitigation strategy. *PLoS ONE* **2013**, *8*. [[CrossRef](#)]
5. Leng, L.; Huang, H.; Li, H.; Li, J.; Zhou, W. Biochar stability assessment methods: A review. *Sci. Total Environ.* **2019**, *647*, 210–222. [[CrossRef](#)]
6. Leng, L.; Xu, X.; Wei, L.; Fan, L.; Huang, H.; Li, J.; Zhou, W. Biochar stability assessment by incubation and modelling: Methods, drawbacks and recommendations. *Sci. Total Environ.* **2019**, *664*, 11–23. [[CrossRef](#)]
7. Leng, L.; Huang, H. An overview of the effect of pyrolysis process parameters on biochar stability. *Bioresour. Technol.* **2018**, *270*, 627–642. [[CrossRef](#)] [[PubMed](#)]
8. Cross, A.; Sohi, S.P. A method for screening the relative long-term stability of biochar. *GCB Bioenergy* **2013**, *5*, 215–220. [[CrossRef](#)]
9. Mašek, O.; Brownsort, P.; Cross, A.; Sohi, S. Influence of production conditions on the yield and environmental stability of biochar. *Fuel* **2013**, *103*, 151–155. [[CrossRef](#)]
10. Crombie, K.; Mašek, O.; Sohi, S.P.; Brownsort, P.; Cross, A. The effect of pyrolysis conditions on biochar stability as determined by three methods. *GCB Bioenergy* **2013**, *5*, 122–131. [[CrossRef](#)]
11. Yang, F.; Zhao, L.; Gao, B.; Xu, X.; Cao, X. The interfacial behavior between biochar and soil minerals and its effect on biochar stability. *Environ. Sci. Technol.* **2016**, *50*, 2264–2271. [[CrossRef](#)]
12. Jindo, K.; Mizumoto, H.; Sawada, Y.; Sanchez-Monedero, M.A.; Sonoki, T. Physical and chemical characterization of biochars derived from different agricultural residues. *Biogeosciences* **2014**, *11*. [[CrossRef](#)]
13. Santín, C.; Doerr, S.H.; Merino, A.; Bucheli, T.D.; Bryant, R.; Ascough, P.; Masiello, C.A. Carbon sequestration potential and physicochemical properties differ between wildfire charcoals and slow-pyrolysis biochars. *Sci. Rep.* **2017**, *7*, 1–11. [[CrossRef](#)] [[PubMed](#)]
14. Plante, A.F.; Fernández, J.M.; Leifeld, J. Application of thermal analysis techniques in soil science. *Geoderma* **2009**, *153*, 1–10. [[CrossRef](#)]
15. Zimmerman, A.R. Abiotic and microbial oxidation of laboratory-produced black carbon (Biochar). *Environ. Sci. Technol.* **2010**, *44*, 1295–1301. [[CrossRef](#)] [[PubMed](#)]
16. Wang, J.; Xiong, Z.; Kuzyakov, Y. Biochar stability in soil: Meta-analysis of decomposition and priming effects. *GCB Bioenergy* **2016**, *8*, 512–523. [[CrossRef](#)]
17. Kuzyakov, Y.; Subbotina, I.; Chen, H.; Bogomolova, I.; Xu, X. Black carbon decomposition and incorporation into soil microbial biomass estimated by <sup>14</sup>C labeling. *Soil Biol. Biochem.* **2009**, *41*, 210–219. [[CrossRef](#)]
18. Restuccia, F.; Mašek, O.; Hadden, R.M.; Rein, G. Quantifying self-heating ignition of biochar as a function of feedstock and the pyrolysis reactor temperature. *Fuel* **2019**, *236*, 201–213. [[CrossRef](#)]
19. Backer, R.; Ghidotti, M.; Schwinghamer, T.; Saeed, W.; Grenier, C.; Dion-Laplante, C.; Smith, D.L. Getting to the root of the matter: Water-soluble and volatile components in thermally-treated biosolids and biochar differentially regulate maize (*Zea mays*) seedling growth. *PLoS ONE* **2018**, *13*, 1–18. [[CrossRef](#)] [[PubMed](#)]
20. Suthar, R.; Wang, C.; Nunes, M.; Chen, J.; Sargent, S.; Bucklin, R.; Gao, B. Bamboo biochar pyrolyzed at low temperature improves tomato plant growth and fruit quality. *Agriculture* **2018**, *8*, 153. [[CrossRef](#)]
21. Peng, X.; Ye, L.L.; Wang, C.H.; Zhou, H.; Sun, B. Temperature- and duration-dependent rice straw-derived biochar: Characteristics and its effects on soil properties of an Ultisol in southern China. *Soil Till. Res.* **2011**, *112*, 159–166. [[CrossRef](#)]
22. Sun, D.; Lan, Y.; Xu, E.G.; Meng, J.; Chen, W. Biochar as a novel niche for culturing microbial communities in composting. *Waste Manag.* **2016**, *54*, 93–100. [[CrossRef](#)] [[PubMed](#)]
23. Knoblauch, C.; Maarifat, A.A.; Pfeiffer, E.M.; Haeefe, S.M. Degradability of black carbon and its impact on trace gas fluxes and carbon turnover in paddy soils. *Soil Biol. Biochem.* **2010**, *43*, 1768–1778. [[CrossRef](#)]

24. Liu, Y.; Lu, H.; Yang, S.; Wang, Y. Impacts of biochar addition on rice yield and soil properties in a cold waterlogged paddy for two crop seasons. *Field Crop Res.* **2016**, *191*, 161–167. [[CrossRef](#)]
25. Liu, Y.; Yang, S.; Lu, H.; Wang, Y. Effects of biochar on spatial and temporal changes in soil temperature in cold waterlogged rice paddies. *Soil Tillage Res.* **2018**, *181*, 102–109. [[CrossRef](#)]
26. Wang, C.; Liu, J.; Shen, J.; Chen, D.; Li, Y.; Jiang, B.; Wu, J. Effects of biochar amendment on net greenhouse gas emissions and soil fertility in a double rice cropping system: A 4-year field experiment. *Agric. Ecosyst. Environ.* **2018**, *262*, 83–96. [[CrossRef](#)]
27. Enders, A.; Hanley, K.; Whitman, T.; Joseph, S.; Lehmann, J. Characterization of biochars to evaluate recalcitrance and agronomic performance. *Bioresour. Technol.* **2012**, *114*, 644–653. [[CrossRef](#)]



© 2019 by the authors. Licensee MDPI, Basel, Switzerland. This article is an open access article distributed under the terms and conditions of the Creative Commons Attribution (CC BY) license (<http://creativecommons.org/licenses/by/4.0/>).